Available online at www.sciencedirect.com
SCIENCE DIRECT®
Carbohydrate Research 340 (2005) 875–879
Carbohydrate RESEARCH

Ramachandran free-energy surfaces for disaccharides: trehalose, a case study

Michelle M. Kuttel[a,b] and Kevin J. Naidoo[a,c,*]

[a]*Department of Chemistry, University of Cape Town, Cape Town, South Africa*
[b]*Department of Computer Science, University of Cape Town, Cape Town, South Africa*
[c]*Centre for High Performance Computing, Western Cape, South Africa*

Received 19 October 2004; accepted 10 January 2005

In honour of Professor David A. Brant

Abstract—We present calculated potential of mean force surfaces for rotation about ϕ, ψ dihedral angles of the α(1↔1)α-glycosidic linkage in the disaccharide trehalose (α-D-Glc-(1↔1)-α-D-Glc) in both vacuum and aqueous solution. The effects of aqueous solvation upon the α(1↔1)α-glycosidic linkage are investigated through comparison of the vacuum and aqueous solution free-energy surfaces. These surfaces reveal that trehalose is restricted to a single minimum-energy conformation in both vacuum and solution. The exceptional rigidity of this disaccharide in solution may provide a molecular rationale for the antidesiccant properties of trehalose glasses.

Keywords: Trehalose; Free-energy calculations; Adaptive umbrella sampling; Conformational transitions

1. Introduction

The non-reducing disaccharide α,α-trehalose (α-D-Glc*p*-(1↔1)-α-D-Glc*p*) is of interest principally because it is the most potently active cryoprotective and antidesiccant disaccharide known. It is the major blood sugar in most insects and is found in large concentrations in a variety of organisms adapted to periods of cold and drought, such as Baker's yeast.

The α,α-trehalose disaccharide is naturally far more abundant than its α,β-trehalose and β,β-trehalose isomers and will be referred to here simply as trehalose. The glycosidic linkage conformation in trehalose is described by the ϕ and ψ dihedral angles, though in this case the two angles are symmetrically equivalent. This disaccharide is relatively rigid, as the combination of two axial bonds together with the close proximity of the hydroxymethyl groups drastically reduces the conformational space available to its glycosidic linkage. Further, α,α-trehalose has a significantly higher glass-transition temperature at all water contents than other disaccharide–water systems.[1] Crystal structures[2,3] and solution experiments[4–6] have shown trehalose to adopt a single conformation. This is supported by several computational studies, particularly Molecular Modelling adiabatic map calculations[7–10] and Molecular Dynamics simulations of trehalose in aqueous solution.[9–14] Experiment and computer simulations have shown trehalose to affect the hydrogen-bonding network of the surrounding water molecules.[9,15] A study by Englesen et al. found that the hydration states of trehalose in the solid and liquid state were similar.[10] The molecular mechanism behind the antidesiccant properties of trehalose has still to be established, though a recent hypothesis on the basis of the available experimental evidence suggests a gradual formation of dihydrate trehalose crystals followed by final dehydration.[16]

Theoretical calculations in the form of Ramachandran, or adiabatic, contour maps of the conformational energy as a function of the glycosidic torsion angles, ϕ

* Corresponding author. Fax: +27 21 689 7499; e-mail: knaidoo@science.uct.ac.za

0008-6215/$ - see front matter © 2005 Elsevier Ltd. All rights reserved.
doi:10.1016/j.carres.2005.01.031

and ψ, are often used to assess the conformational space of disaccharides[17–19] and have been shown to be useful for estimating polysaccharide conformation.[20,18] Though adiabatic maps are useful in this regard, ultimately an investigation of the effect of solution on the glycosidic linkage is required. Potential of mean force (PMF) calculations for a glycosidic linkage provide a complete description of the preferred conformation and the structural fluctuations that a disaccharide is likely to undergo. If glycosidic linkages are assumed to operate independently of each other, a 2D PMF for the glycosidic linkage in a disaccharide will also provide all the information required to determine the average chain conformation of a homopolysaccharide, as well as the dynamic behaviour of the chain.[19] In addition, if performed in solution, PMF calculations reveal the effect of solvent on the properties of the linkage (Fig. 1).

Though valuable, PMF calculations in solution are rarely undertaken because of their computational complexity and the time required to average over all solvent and solute configurations. We have recently developed an adaptive umbrella sampling protocol for calculating free-energy surfaces for dihedral rotations.[21] Here we use this method to calculate two-dimensional ϕ, ψ potential of mean force energy surfaces for the trehalose in both vacuum and solution. In addition, novel one-dimensional free-energy surfaces for rotation about the $\alpha(1\rightarrow1)\alpha$ glycosidic linkage were calculated from the 2D ϕ, ψ PMFs. Free-energy surfaces for the glycosidic linkage in trehalose establish the minimum energy conformation and the entire range of mobility of this disaccharide in solution, and hence may facilitate understanding of the molecular and thermodynamic origins of its cryoprotective properties.

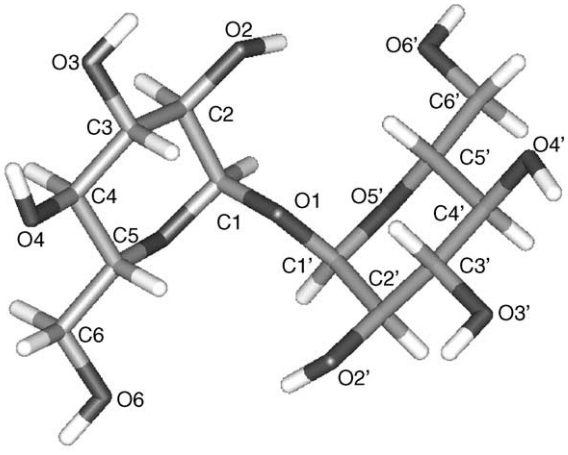

Figure 1. A minimised three-dimensional structure of the α,α-trehalose disaccharide, showing the atomic naming scheme.

2. Computational methods

The principal degrees of freedom for trehalose are the symmetrically equivalent torsion angles, ϕ = H-1–C-1–O-1–C-1′ and ψ = C-1–O-1–C-1′–H-1′. These definitions for ϕ and ψ are analogous to ϕ_H and ψ_H in IUPAC convention. In this work, a further dihedral, τ, is defined as: τ = H-1–C-1–C-1′–H-1′. This non-IUPAC dihedral angle describes rotation about a virtual C-1–C-1 bond. The value of τ is simply the sum of ϕ and ψ and it is thus a one-dimensional measure of the relative orientation of the glucose subunits involved in the glycosidic linkage.

The 2D ϕ, ψ PMF for trehalose in vacuum and solution was calculated using an iterative adaptive umbrella sampling method.[21] The $360° \times 360°$ umbrella potential surface for the two glycosidic linkage dihedral angles was represented as a two-dimensional grid of points, with a grid separation of 2.5°. At each integration step of a simulation, the biasing potential energy to be applied to the current ϕ, ψ position was calculated from a cubic spline of the umbrella energy surface. After each simulation, a two-dimensional ϕ, ψ distribution histogram was calculated by summing the number of configurations in each $2.5° \times 2.5°$ bin over the production phase of the trajectory. The Weighted Histogram Analysis Method (WHAM) was then applied, using a tolerance value of 0.001, to obtain an optimum combination of the all the simulations distributions and thus the next estimate of the PMF. This PMF surface was extrapolated into unexplored regions by setting unsampled bins to the maximum value of the sampled bins. The resultant PMF surface was smoothed three times. Subsequently, regions in the 2D ϕ, ψ PMF associated with high-energy steric clashes of the atoms were removed. This was done by setting any bin in the PMF with an energy value greater than a predetermined cut-off of 20 kcal/mol to the cut-off value. The umbrella potential for the next simulation was set to the negative of this PMF estimate.

Each umbrella simulation began with an equilibrium phase of 500 ps, followed by a production phase ranging from 2 to 20 ns in length. Only the production phase was used to calculate the simulation distribution. Successive simulations in a series were gradually run for longer periods as the PMF estimates improved and more of the phase space was explored. The first simulation in each series was started from a minimised and equilibrated coordinate set and performed with a flat umbrella potential surface. Subsequent simulations were begun from the final conformation of the previous simulation, to facilitate gradual exploration of the whole of conformational space. After every eight simulations, the next simulation was begun from the original equilibrated starting configuration. Convergence of the whole adaptive umbrella sampling procedure was defined to occur when, for a single simulation, every bin k in $n_{j,k}$ in the

ϕ, ψ range of interest was occupied at least once. Up to 200 simulations were used to obtain the final PMF, but at any time not more than the latest 50 distributions were used to estimate the next PMF; earlier simulations were gradually discarded as new, more extensive distributions were produced. A total of approximately 500 ns of simulation time was required to produce each of the final PMF surfaces. The 1D τ PMF for trehalose was calculated by summing all the contributing ϕ, ψ pair populations (obtained from the 2D ϕ, ψ PMFs) for each τ value. The τ PMF was then calculated from the normalised τ population distribution.

2.1. Simulation conditions

Molecular dynamics simulations were performed using the program CHARMM[22] (version 27b1), with modifications incorporated into the USERE module in order to implement both the two-dimensional adaptive umbrella sampling PMF calculations and the stretching simulations. The CSFF carbohydrate parameter set[21] for the CHARMM force field was used to represent the carbohydrate molecules in all the simulations. The TIP3P model was used to represent water.

For the solution simulations, the trehalose disaccharide was placed in a previously equilibrated cube of 512 TIP3P waters. Solvent water molecules that overlapped with the solute molecule were removed and the system was equilibrated for 500 ps. The solution simulation surrounded the trehalose disaccharide with 489 TIP3P water molecules[23] in a cube of length 24.64 Å. This gives a density of 1.013 g/cm^3. The cube was subjected to minimum image periodic boundary conditions to eliminate edge effects.

Initial velocities for the atoms were selected at random from a Boltzmann distribution at 300 K. All simulations were performed in the canonical ensemble (constant n, V, T), using stochastic Langevin dynamics with a frictional coefficient of 62.5 to maintain a constant temperature of 300 K. The equations of motion were integrated using a Leap-Frog Verlet integrator[24] with a step size of 1 fs. The SHAKE algorithm[25] was used to fix the length of bonds involving hydrogen atoms and the water molecule geometry throughout each simulation. Non-bonded interactions were truncated using a switching function applied on a neutral group basis between 10.0 and 12.0 Å. The groups corresponded to electrically neutral collections of atoms in the carbohydrate molecules and entire water molecules for the solvent.

3. Results and discussion

The vacuum PMF for trehalose, shown in Figure 2a, has a symmetrical shape similar to published adiabatic maps,

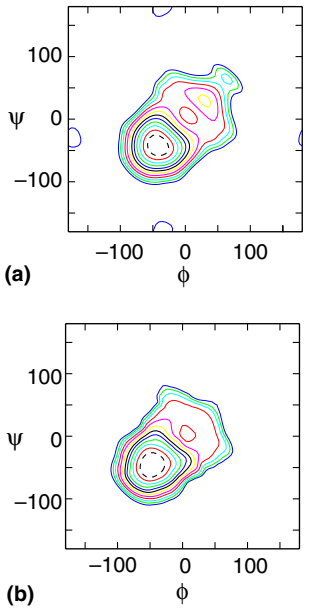

Figure 2. Contoured ϕ, ψ free-energy surfaces for trehalose (a) in vacuum and (b) TIP3P water solution. In each case, contours appear at 1 kcal/mol intervals above the global energy minimum, to a maximum of 12 kcal/mol. Contours higher than this are not shown. The 1 kcal/mol contour is shown as a dashed line.

the diagonal symmetry of the map being a consequence of the molecular symmetry. The global energy minimum is a *gauche* conformation situated at ϕ, $\psi = -40.0°$, $-42.5°$ on the vacuum map and ϕ, $\psi = -45.0°$, $-45.0°$ on the solution map. Crystal structures of trehalose show an asymmetric extended *gauche* conformation with ϕ, $\psi = -58°$, $-45°$; which is stabilised by an O-6–O-2′ hydrogen bond with the primary alcohols in *gt* conformations.[2,3] Experiments in solution have revealed similar *gauche* conformations: optical rotation experiments show ϕ, $\psi = -60°$, $-60° \pm 5°$[4,5] and NMR proton–carbon coupling measurements have ϕ, $\psi = -41°$, $-41° \pm 5°$.[6] Therefore, the global minima for both the vacuum and solution PMFs are in the region of the crystal and solution structures. Adiabatic maps calculated for trehalose using the MM3[8] and MM2CARB[7] force fields as well as quantum mechanical methods[26] have also identified this region as the global energy minimum.

However, both of the previously published adiabatic map calculations using CHARMM force fields[9,10] contradict experimental data in identifying a *trans* global minimum-energy configuration near ϕ, $\psi = 60°$, $60°$. In particular, the minimum energy structure identified using the HGFB force field had the primary alcohols in the trans *tg* conformation.[9] As the HGFB force field has been shown to favour the *tg* conformation,[21] this suggests that accurate parameterisation of the primary alcohol is necessary for identification of the correct global energy minimum in trehalose. The quantum mechanical study by French et al. calculated the energy difference between the *gauche* and *trans* conformations

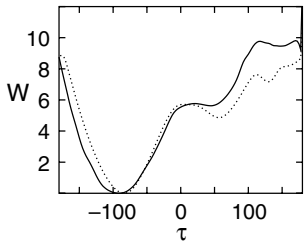

Figure 3. PMF surfaces for the α,α-trehalose τ dihedral in vacuum (dotted line) and solution (solid line) obtained from the ϕ, ψ populations. The graphs are shown relative to their global energy minima, with the energy in kcal/mol.

to be 5–7 kcal/mol.[26] This is in agreement with the vacuum PMF surface shown here, which has a *gauche–trans* energy difference of 7 kcal/mol. However, the valley at approximately ϕ, $\psi = 0°$, 0° is 8 kcal/mol higher than in the French et al. study.

The solution and vacuum PMFs calculated here for trehalose are remarkably similar. The glycosidic linkage conformation of trehalose is largely unaffected by the surrounding water molecules. This is in contrast to the (1→4)-linkage in the maltose (4-*O*-α-D-glucopyranosyl-D-glucopyranose) and dixylose disaccharides (4-*O*-α-D-xylopyranosyl-α-D-xylopyranose).[27–31] In fact, the water solvent actually favours this conformation, as can be easily seen in a comparison of the 1D τ PMFs for solution and vacuum shown in Figure 3. Solvation increases the preference for the central energy region by raising the energy of the high valleys at ϕ, $\psi = 30°$, 30° and ϕ, $\psi = 65°$, 65°. These more compact conformations are sterically strained and their stabilising interresidue hydrogen bonds are disrupted by the aqueous solution. Trehalose is thus quite rigid in water. This results in the location of the oxygen atoms being essentially fixed in relation to one another, which may result in the structure that MD simulations have shown trehalose to impose on the surrounding water solution.[9]

4. Conclusions

We have presented complete free-energy surfaces for rotation about the trehalose α(1↔1)α linkage in both vacuum and aqueous solution. These reveal that global energy minimum found for the trehalose disaccharide has the same location in vacuum as in solution. Encouraging support for the correct parameterisation of the hydroxymethyl dihedral angles is given by the fact that this is the first CHARMM force field to produce a minimum-energy conformation in agreement with crystal structures and NMR solution experiments. Trehalose is shown to have a very limited range of motion about the minimum-energy conformation in both vacuum and solution. Comparison of the solution and vacuum PMFs showed that aqueous solution restricts the low-energy conformations for trehalose. This rigidity in solution may result in the high glass-transition temperature and marked antidesiccant properties of trehalose.

Acknowledgements

M.K. thanks the National Research Foundation (NRF Pretoria) for doctoral support. K.J.N. thanks the United States Department of Agriculture (USA) for support (USDA-ARS grant no. 58-4012-5-F120).

References

1. Chen, A. F. T.; Toner, M. Literature review: Supplemented phase diagram of the trehalose water binary mixture. *Cryobiology* **2000**, *40*, 277–282.
2. Brown, G. M.; Rohrer, D. C.; Berking, B.; Beevers, C. A.; Gould, R. O.; Simpson, R. *Acta Crystallogr.* **1972**, 3145–3158.
3. Jeffrey, G. A.; Nanni, R. *Carbohydr. Res.* **1985**, *137*, 21–30.
4. Duda, C. A.; Stephens, E. S. *J. Am. Chem. Soc.* **1990**, *112*, 7406.
5. Duda, C. A.; Stephens, E. S. *J. Am. Chem. Soc.* **1993**, *115*, 8487.
6. Batta, G.; Kövér, K. E.; Gervay, J.; Horyák, M.; Roberts, G. M. *J. Am. Chem. Soc.* **1997**, *119*, 1336–1345.
7. Tvaroška, I.; Vaclavik, L. *Carbohydr. Res.* **1987**, *160*, 137–149.
8. Dowd, M. K.; Reilly, P. J.; French, A. D. *J. Comput. Chem.* **1992**, *13*(1), 102–114.
9. Liu, Q.; Schmidt, R. K.; Teo, B.; Karplus, P. A.; Brady, J. W. *J. Am. Chem. Soc.* **1997**, *119*(33), 7851–7862.
10. Engelsen, S. B.; Pérez, S. *J. Phys. Chem. B* **2000**, *104*, 9301–9311.
11. Donnamaria, M. C.; Howard, E. I.; Grigera, J. R. *J. Chem. Soc., Faraday Trans.* **1994**, *90*(18), 2731–2735.
12. Sakurai, M.; Murata, M.; Inoue, Y.; Hino, A.; Kobayashi, S. *Bull. Chem. Soc. Jpn.* **1997**, *70*(4), 847–858.
13. Bonanno, G.; Noto, R.; Fornili, S. L. *J. Chem. Soc., Faraday Trans.* **1998**, *94*(18), 2755–2762.
14. Conrad, P. B.; Pablo, J. J. *J. Phys. Chem. A* **1999**, *103*, 4049–4055.
15. Cesàro, A.; Magazù, V.; Migliardo, F.; Sussich, F.; Vadalà, M. *Physica B* **2004**, *350*, e367–e370.
16. Sussich, F.; Skopec, C.; Brady, J. W.; Cesàro, A. *Carbohydr. Res.* **2001**, *334*, 165–176.
17. Brant, D. A.; Liu, H.-S.; Zhu, Z. S. *Carbohydr. Res.* **1995**, *278*, 11–26.
18. Brant, D. A. *Pure Appl. Chem.* **1997**, *69*(9), 1885–1892.
19. Perico, A.; Mormino, M.; Urbani, R.; Cesàro, A.; Tylianakis, E.; Dais, P.; Brant, D. A. *J. Phys. Chem. B* **1999**, *103*, 8162–8171.
20. Brant, D. A.; Dimpfl, W. L. *Macromolecules* **1970**, *3*(5), 655–665.
21. Kuttel, M.; Brady, J. W.; Naidoo, K. J. *J. Comput. Chem.* **2002**, *23*(13), 1236–1243.
22. Brooks, B. R.; Bruccoleri, R. E.; Olafson, B. D.; States, D. J.; Swaminathan, S.; Karplus, M. *J. Comput. Chem.* **1983**, *4*(2), 187–217.

23. Jorgensen, W. L.; Chandrasekhar, J.; Madura, J. D.; Impey, R. W.; Klein, M. L. *J. Chem. Phys.* **1983**, *79*(2), 926–935.
24. Hockney, R. W. *Methods Comput. Phys.* **1970**, *9*, 136–211.
25. Ryckaert, J. P.; Ciccotti, G.; Berendsen, H. J. C. *J. Comput. Phys.* **1977**, *23*, 327–341.
26. French, A. D.; Johnson, G. P.; Kelterer, A.-M.; Dowd, M. K.; Cramer, C. J. *J. Phys. Chem. A* **2002**, *106*, 4988–4997.
27. Ha, S. N.; Giammona, A.; Field, M.; Brady, J. W. *Carbohydr. Res.* **1988**, *180*, 207–221.
28. Glennon, T. M.; Zheng, Y.; le Grand, S. M.; Shutzberg, B. A.; Merz, K. M. J. *J. Comput. Chem.* **1994**, *15*(9), 1019–1040.
29. Ott, K.; Meyer, B. *Carbohydr. Res.* **1996**, *281*, 11–34.
30. Naidoo, K. J.; Brady, J. W. *J. Am. Chem. Soc.* **1999**, *121*(10), 2244–2252.
31. Naidoo, K. J.; Kuttel, M. *J. Comput. Chem.* **2001**, *22*(4), 445–456.